JOURNAL OF SOLID STATE CHEMISTRY **134,** 326–331 (1997)
ARTICLE NO. SC977565

Crystal Structure, Specific Heat, and ^{119}Sn Mössbauer Spectroscopy of $CeRu_4Sn_6$: A Ternary Stannide with Condensed, Distorted $RuSn_6$ Octahedra

R. Pöttgen,*,[1] R.-D. Hoffmann,* E. V. Sampathkumaran,† I. Das,†,[2] B. D. Mosel,‡ and R. Müllmann‡

*Anorganisch-Chemisches Institut, Universität Münster, Wilhelm-Klemm-Straße 8, D-48149 Münster, Germany; † Tata Institute of Fundamental Research, Homi Baba Road, Colaba, Bombay 400 005, India; and ‡ Institut für Physikalische Chemie, Universität Münster, Schloßplatz 4/7, D-48149 Münster, Germany

Received May 1, 1997; accepted July 17, 1997

$CeRu_4Sn_6$ was prepared from the elements by a reaction in an arc-melting furnace and subsequent annealing at 1123 K. It crystallizes with the tetragonal YRu_4Sn_6 type structure of space group $I\bar{4}2m$: $a = 688.1(1)$, $c = 975.2(2)$ pm, $V = 0.4617(1)$ nm^3, w$R2 = 0.0472$, 554 F^2 values, and 19 variables. The cerium atoms in $CeRu_4Sn_6$ have coordination number 16 formed by 12 tin and 4 ruthenium atoms. These polyhedra are arranged in a tetragonal body-centered packing and are linked by common Sn1 atoms. The strongest bonding interactions are between ruthenium and tin atoms. The ruthenium atoms have 6 tin neighbors at distances from 256.9 to 276.8 pm in the form of a strongly distorted octahedron. Four of such octahedra are condensed via common edges and faces forming $[Ru_4Sn_6]$ units. These groups are packed in a tetragonal body-centered arrangement. The cerium atoms occupy the space between the $[Ru_4Sn_6]$ units. The $[Ru_4Sn_6]$ substructure of $CeRu_4Sn_6$ is discussed in comparison with the structures of Ru_2Sn_3, $LaRuSn_3$, and $Ru_3Sn_{15}O_{14}$ which also contain condensed $RuSn_6$ octahedra or trigonal prisms as characteristic structural motifs. Despite the two different tin sites the ^{119}Sn Mössbauer spectroscopic measurements show only one signal at $\delta = 1.99$ mm/s subjected to quadrupole splitting. Heat capacity measurements indicate that $CeRu_4Sn_6$ behaves like a heavy-fermion compound.

Key Words: **$CeRu_4Sn_6$; stannide; cerium intermetallics.**

INTRODUCTION

The binary system ruthenium–tin was intensively investigated in the past (1–4). It is characterized by the stannides Ru_3Sn_7 (cubic Ir_3Ge_7-type; 5, 1, 7) and Ru_2Sn_3 (tetragonal Ru_2Si_3-type; 1, 6, 7). Ru_3Sn_7 melts congruently at 1530(±5) K, while Ru_2Sn_3 decomposes by a peritectic reaction at 1539(±4) K (4). A very recent reinvestigation of Ru_2Sn_3 by temperature-dependent X-ray data (7) showed a phase transition between 240 and 100 K. A Rietveld analysis (7) of the low-temperature (LT) structure of Ru_2Sn_3 confirmed isotypism with the LT-Ru_2Si_3-type (8). This phase transition is also supported by the temperature dependence of the specific resistivity.

When it comes to the structural characterization of ternary rare-earth and actinoid ruthenium stannides, however, our knowledge is quite limited. The only actinoid ruthenium stannide known is the 53 K ferromagnet URuSn (9) which crystallizes with the ZrNiAl-type structure, a ternary ordered version of Fe_2P. With the early rare-earth elements the stannides LnRuSn$_3$ (Ln = La–Nd) are formed (10, 11). They crystallize with a site occupancy variant of the $Yb_3Ru_4Sn_{13}$ type (12). Several tin-rich rare-earth ruthenium tin alloys have been prepared in the 1980s (13–16) when searching for new superconducting materials. These alloys have structures related to $Tb_5Rh_6Sn_{18}$ (17, 18).

With yttrium the metallic stannide YRu_4Sn_6 (19) has recently been reported. In a previous paper we communicated the magnetic and electrical properties of isotypic $CeRu_4Sn_6$ (20) which exhibits the characteristics of a dense Kondo system. Herein we report on the structure refinement from single-crystal X-ray data and an investigation of the specific heat and ^{119}Sn Mössbauer spectroscopy of this stannide.

EXPERIMENTAL

Starting materials for the preparation of $CeRu_4Sn_6$ were ingots of cerium, ruthenium powder, and tin granules, all with stated purities better than 99.9%. The elemental components were arc-melted in a water-cooled copper crucible under an argon atmosphere. The sample was remelted several times to ensure homogeneity. The weight losses during the melting procedures were negligible. The molten ingot

[1] To whom correspondence should be addressed.
[2] Present address: IUC Indore, Khandwa Road, Indore 1, India.

0022-4596/97 $25.00

was subsequently annealed in an evacuated sealed silica tube at 1123 K for 5 days and quenched in air.

The purity of the sample was checked by a Guinier powder pattern using Cu$K\alpha_1$ radiation and α-quartz (a = 491.30, c = 540.46 pm) as an internal standard. The lattice constants (Table 1) were obtained by a least-squares refinement of the powder data. The indexing of the diffraction lines was facilitated by an intensity calculation (21) using the positional parameters of the refined structure.

The homogeneity of the sample was analyzed by EDX measurements using a Leica 420 I scanning electron microscope with ruthenium, tin, and CeO_2 as standards. The composition of our sample was very close to $CeRu_4Sn_6$ and the Ru/Sn ratio did not vary significantly from 4 : 6. The sample of this investigation is identical to the sample of the earlier electrical resistivity and magnetic susceptibility studies (20).

Single-crystal intensity data were collected by use of a four-circle diffractometer (Enraf–Nonius CAD4) with graphite monochromatized Mo$K\alpha$ radiation and a scintillation counter with pulse height discrimination. Since the structure determination for the prototype, YRu_4Sn_6 (19), revealed the noncentrosymmetric space group $I\bar{4}2m$ (No. 121), intensity data were collected in one quarter of the reciprocal sphere together with the corresponding Friedel reflections. Reflections corresponding to a primitive lattice ($h + k + l = 2n + 1$) were additionally recorded in the first part of the data collection but no violations of the body centered lattice were found. All relevant data concerning the data collection are listed in Table 1.

Specific heat data were measured between 2 and 80 K by a semiadiabatic heat pulse method employing a self-fabricated setup (21).

^{119}Sn Mössbauer spectroscopic experiments were performed at absorber temperatures between 300 and 4.2 K on the same polycrystalline sample used for the heat capacity measurement. The $Ca^{119m}SnO_3$ source was held at room temperature and a palladium foil of 0.05 mm thickness was used to reduce the tin K X-rays concurrently emitted by the source.

TABLE 1
Crystal Data and Structure Refinement for $CeRu_4Sn_6$

Empirical formula	$CeRu_4Sn_6$
Formula weight	1256.54 g/mol
Temperature	293(2) K
Wavelength	71.073 pm
Crystal system	tetragonal
Space group	$I\bar{4}2m$ (No. 121)
Unit-cell dimensions	a = 688.1(1) pm
(Guinier powder data)	c = 975.2(2) pm
	V = 0.4617(1) nm^3
Formula units per cell	Z = 2
Calculated density	9.04 g/cm^3
Crystal size	15 · 30 · 30 μm^3
Data collection method	Enraf–Nonius, CAD4
Absorption correction	from ψ-scan data
Transmission ratio (max/min)	1.000 : 0.567
Absorption coefficient	27.0 mm^{-1}
F(000)	1068
θ range for data collection	2° to 35°
Scan type	$\omega/2\theta$
Range in hkl	±11, ±9, ±15
Total number of reflections	2408
Independent reflections	554 (R_{int} = 0.0596)
Reflections with $I > 2\sigma(I)$	510 (R_{sigma} = 0.0371)
Refinement method	Full-matrix least-squares on F^2
Data/restraints/parameters	554/0/19
Goodness-of-fit on F^2	1.127
Final R indices [$I > 2\sigma(I)$]	$R1$ = 0.0220, w$R2$ = 0.0454
R indices (all data)	$R1$ = 0.0282, w$R2$ = 0.0472
Extinction coefficient	0.0011(1)
Absolute structure parameter	0.00(6)
Largest differential peak and hole	1782 and −2053 e/nm^3

RESULTS AND DISCUSSION

Powders and single crystals of $CeRu_4Sn_6$ are light gray and stable in air over long periods of time. No decomposition whatsoever was observed after several months. The irregular-shaped single crystals exhibit silvery metallic luster.

Structure Refinement

Single crystals of $CeRu_4Sn_6$ were isolated from the crushed sample after the annealing process and examined by Buerger precession photographs to establish both symmetry and suitability for intensity data collection. The photographs (reciprocal layers $hk0$, $hk1$, and $h0l$) showed the high tetragonal Laue symmetry $4/mmm$ and the only systematic extinctions were those for a body-centered lattice. This led to the space groups $I4/mmm$, $I4mm$, $I\bar{4}2m$, and $I\bar{4}m2$, of which the noncentrosymmetric group $I\bar{4}2m$ was found to be correct in agreement with the previous results for the yttrium compound (19). All relevant crystallographic data and experimental details are listed in Table 1.

The starting atomic positions were deduced from an automatic interpretation of direct methods with SHELX-86 (22) and the structure was successfully refined using SHELXL-93 (23), with anisotropic displacement parameters for all atoms. In an early stage of the refinement the Flack parameter (24, 25) had a value of about 1.0 indicating the wrong absolute structure. The atomic parameters were subsequently inverted and the correct absolute structure was refined. As a check for the correct composition, the occupancy parameters were refined in a separate series of least-squares cycles. No deviation from full occupancies was observed (Table 2) and the ideal values were assumed again in the final cycles.

TABLE 2
Atomic Coordinates and Isotropic Displacement Parameters (pm^2) for $CeRu_4Sn_6$

Atom	$I\bar{4}2m$	occupancy	x	y	z	U_{eq}
Ce	2*a*	1.000(1)	0	0	0	90(2)
Ru	8*i*	0.999(1)	0.82938(7)	*x*	0.42107(6)	50(1)
Sn1	8*i*	0.995(1)	0.82134(6)	*x*	0.70476(5)	71(1)
Sn2	4*c*	0.992(1)	0	1/2	0	71(2)

Note. U_{eq} is defined as one third of the trace of the orthogonalized U_{ij} tensor. The occupancy parameters were refined in separate least-squares cycles.

TABLE 3
Interatomic Distances (pm) in the Structure of $CeRu_4Sn_6$

Ce:	4	Ru	329.6	Sn1:	1	Ru	256.9
	4	Sn1	336.3		2	Ru	269.9
	4	Sn2	344.0		1	Ru	276.8
	4	Sn1	371.0		2	Sn2	322.3
					1	Ce	336.3
Ru:	1	Sn1	256.9		1	Sn1	347.7
	2	Sn2	266.6		4	Sn1	368.5
	2	Sn1	269.9		1	Ce	371.0
	1	Sn1	276.8		2	Sn2	383.3
	2	Ru	280.8				
	1	Ce	329.6	Sn2:	4	Ru	266.6
	1	Ru	332.1		4	Sn1	322.3
					2	Ce	344.1
					4	Sn1	383.3

Note. All distances shorter than 550 pm (Ce–Ce, Ce–Sn), 465 pm (Ru–Ru, Sn–Sn), and 435 pm (Ce–Ru, Ru–Sn) are listed. Standard deviations are all equal or less than 0.2 pm.

A final difference Fourier synthesis was flat and revealed no significant residual peaks. The results of the refinements are summarized in Table 1. Atomic coordinates and interatomic distances are listed in Tables 2 and 3. Listings of the anisotropic displacement parameters and the observed and calculated structure factors are available.[3]

Crystal Chemistry

The present structure refinement of $CeRu_4Sn_6$ fully confirms the isotypism with the prototype YRu_4Sn_6 (19). The single crystal of the cerium compound had the other handedness when compared with the setting given for YRu_4Sn_6. We therefore list the inverted atomic parameters (Table 2) as obtained from the structure refinement.

As already stated by Venturini *et al.* (19), the YRu_4Sn_6 structure may, from a geometrical point of view, be derived from the well-known Cu_3Au-type structure of YSn_3 by replacing every other yttrium atom by a Ru_4 group in an ordered manner. This replacement results in a larger coordination number (CN) for the rare-earth atoms. In the Cu_3Au type YSn_3 each yttrium atom has 12 tin neighbors forming a regular cuboctahedron, while the coordination number is increased to CN16 (12 Sn + 4 Ru) in the YRu_4Sn_6 structure. These CN16 polyhedra are very regular and packed in a tetragonal body-centered arrangement as outlined for $CeRu_4Sn_6$ in Fig. 1. The CN16 polyhedra are connected via common Sn1 atoms.

In Fig. 2 we show the polyhedra of all atomic sites in a ball–stick presentation. The cerium atoms have CN16 with four ruthenium (329.6 pm), four Sn1 (336.3 pm), four Sn2 (344.0 pm), and four further Sn1 (371.0 pm) atoms in their coordination shell. The wide range of Ce–Sn distances (336.3 to 371.0 pm) nicely reflects the distortions from the ideal Cu_3Au type structure of $CeSn_3$ (26). Here, each cerium atom has an ideal cuboctahedral tin environment with Ce–Sn distances of 333.9 pm. The shorter Ce–Sn1 and Ce–Sn2 distances of 336.3 and 344.0 pm are in the range of the sum of the metallic radii of 344.8 pm for CN12 for

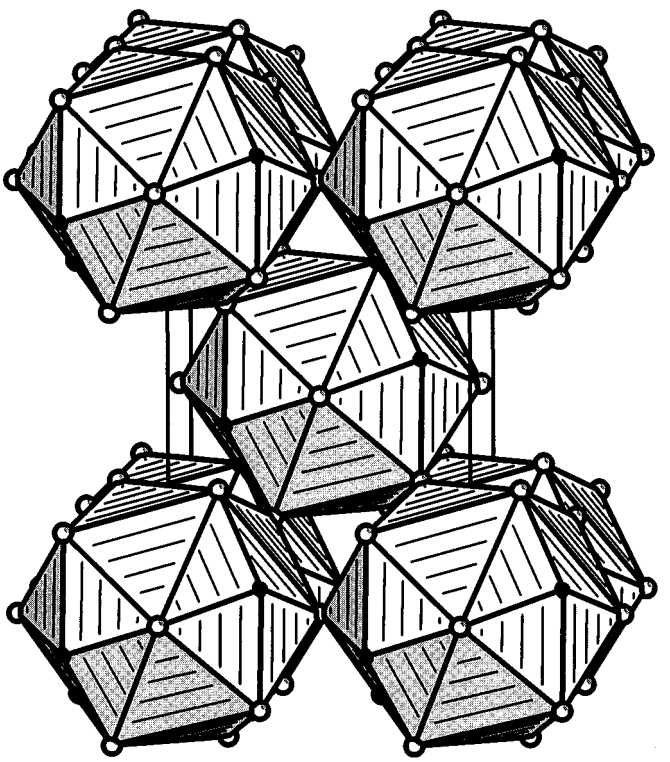

FIG. 1. Crystal structure of $CeRu_4Sn_6$. The CN16 polyhedra (4 Ru (filled circles) + 12 Sn (open circles)) around the cerium atoms are outlined. They are connected via common Sn1 atoms.

[3]Details may be obtained from Fachinformationszentrum Karlsruhe, D-76344 Eggenstein–Leopoldshafen (Germany) by quoting the registry number CSD-406894.

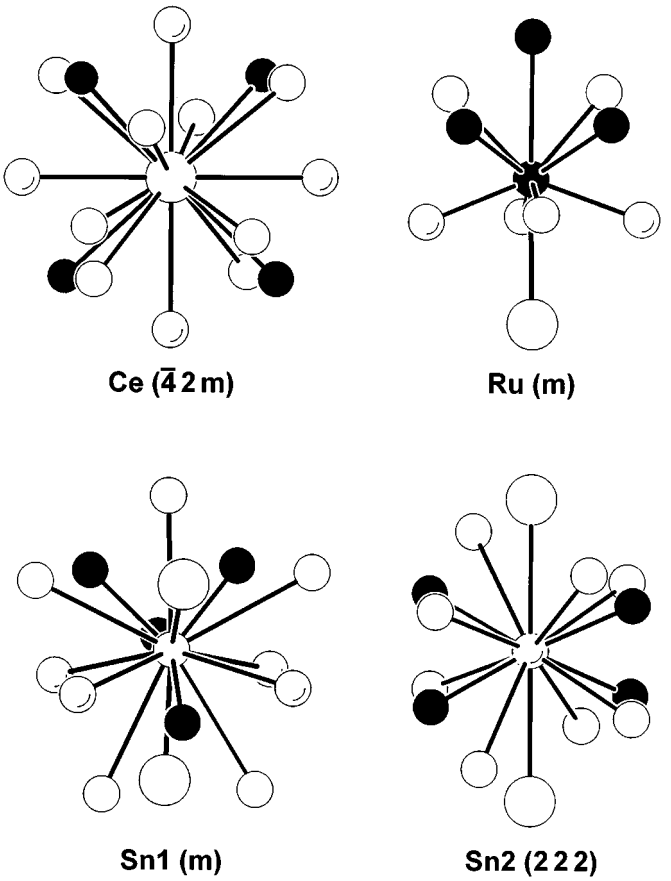

FIG. 2. Coordination polyhedra of $CeRu_4Sn_6$. The site symmetries are given in parentheses.

cerium and tin (27). These Ce–Sn distances also compare well with the Ce–Sn distances in the structures of Ce_2Sn_5 and Ce_3Sn_7 (28, 29) which have structural elements similar to $CeRu_4Sn_6$. The additional four Sn1 atoms at the much longer distance of 371.0 pm still belong to the coordination sphere of the cerium atoms, but the bonding interactions may be considered as very weak.

The ruthenium atoms have CN10 (Fig. 2) with 6 tin (256.9–276.8 pm), 3 ruthenium (2×280.8, 1×332.1 pm), and 1 cerium atom at 329.6 pm in their coordination shell. Since the ruthenium atoms are the smallest atoms in the structure of $CeRu_4Sn_6$, they consequently have the lowest coordination number. The short Ru–Sn distances of 256.9, 266.6, and 269.9 pm are the most remarkable feature of this polyhedron and also of the whole crystal structure. The shortest distance is even shorter than the sum of Paulings single bond radii of 264.5 pm (30) for ruthenium and tin, indicating strong ruthenium–tin bonding interactions.

The tin atoms occupy two crystallographically different sites: 8*i* by Sn1 and 4*c* by Sn2 atoms. The Sn1 atoms have CN15 with 4 ruthenium, 2 cerium, and 9 tin neighbors. The strongest bonding interactions exist certainly between tin and ruthenium with the ruthenium atoms forming a distorted tetrahedron around the Sn1 atoms (Fig. 2). The 9 tin neighbors cover the wide distance range from 322.3 to 383.3 pm. Even the shortest Sn1–Sn2 distance of 322.3 pm is still longer than in white tin (4×302 and 2×318 pm) (31), indicating only very weak tin–tin interactions. Such a wide range of tin–tin contacts is typically observed in binary transition metal stannides (32, 33) and also in Ce_2Sn_5 and Ce_3Sn_7 (28, 29). The Sn2 atoms have only CN14 with 4 ruthenium, 2 cerium, and 8 tin neighbors. Again in this near-neighbor environment the Sn2–Ru interactions at 266.6 pm play the dominant part. However, the Sn–Sn distances show a clear separation in contrast to the Sn1 polyhedra: 4 closer Sn1 neighbors at 322.3 pm and 4 further Sn2 contacts at 383.3 pm.

As already stated above, the ruthenium–tin interactions play an important part in the structure of $CeRu_4Sn_6$. The 6 tin neighbors around each ruthenium atom form a heavily distorted octahedron. Due to the strong distortions, these octahedra have one almost square-like face (top of Fig. 3). The distortion arises by the displacement of one apex. This allows the condensation of four octahedra via two common faces and one common edge forming a $[Ru_4Sn_6]$ cluster unit as outlined in the upper part of Fig. 3. These sphere like $[Ru_4Sn_6]$ units are connected via joint tin atoms building a tetragonal body-centered packing. A cutout of this packing is presented in Fig. 3. The cerium atoms occupy the space between the $[Ru_4Sn_6]$ units. Due to the distortions and the face-sharing of the octahedra, the central ruthenium atoms move toward each other with Ru–Ru distances of 280.8 pm, only somewhat longer than the average Ru–Ru distance of 267.8 pm in *hcp* ruthenium (31). The 4 ruthenium atoms within one $[Ru_4Sn_6]$ cluster unit form a strongly flattened Ru_4 tetrahedron with four weak Ru–Ru interactions. The two longer edges of the flattened tetrahedra have a length of 332.1 pm. These Ru–Ru interactions most likely do not contribute to bonding.

In Fig. 3 the condensed $[Ru_4Sn_6]$ cluster units of $CeRu_4Sn_6$ are compared with several other Ru–Sn substructures of related compounds which are also built up of condensed $RuSn_6$ units. The structure of Ru_2Sn_3 contains 3 crystallographically different ruthenium atoms. Two of these have an octahedral tin environment, while the third is situated in flattened Sn_4 tetrahedra. The $RuSn_6$ octahedra are connected via common edges and corners forming a three-dimensional network. The Ru–Sn distances range from 259 to 282 pm in the octahedra and amount to 264 pm for the tetrahedra. These short Ru–Sn bond lengths indicate strong Ru–Sn bonding in the binary stannide Ru_2Sn_3. This is also the case for the transparent compound $Ru_3Sn_{15}O_{14}$ (34), where the $RuSn_6$ octahedra are condensed via common corners forming one-dimensionally infinite ribbons. A cutout of the $Ru_3Sn_{15}O_{14}$ structure is shown in Fig. 3. The

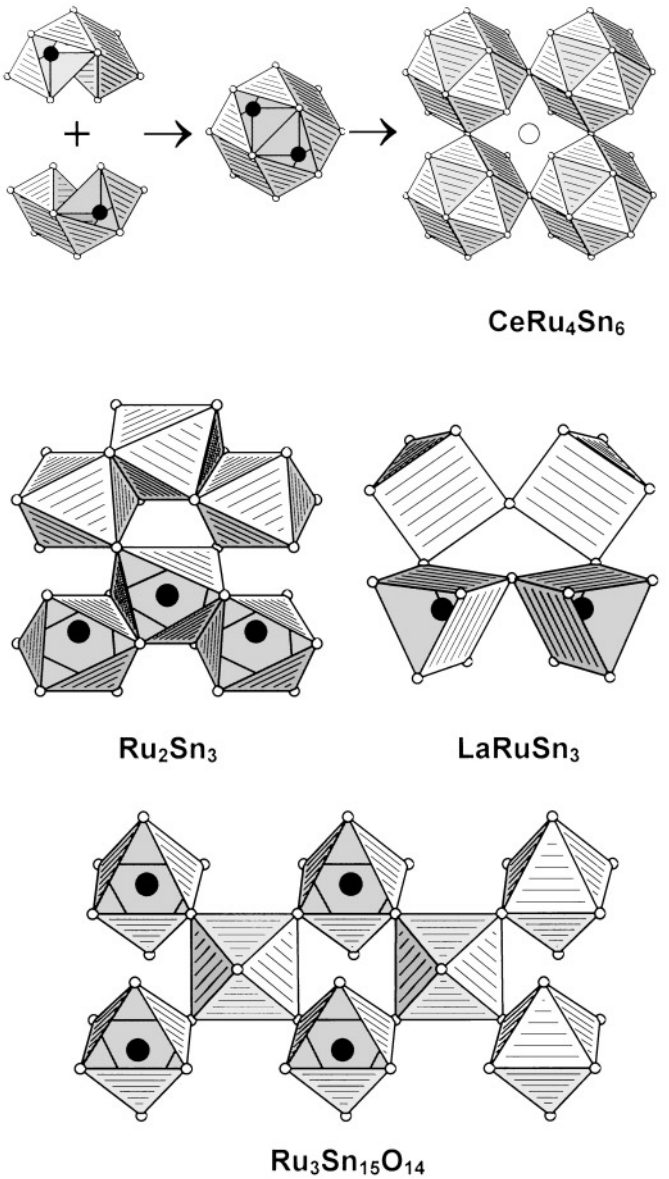

FIG. 3. Cutouts of condensed $RuSn_6$ units in the structures of $CeRu_4Sn_6$, Ru_2Sn_3, $LaRuSn_3$, and $Ru_3Sn_{15}O_{14}$. The tin and ruthenium atoms are shown as small open and filled circles, respectively. The cerium atom of $CeRu_4Sn_6$ is drawn as a large open circle. At the top the condensation mechanism (by face and edge sharing) of four distorted $RuSn_6$ octahedra is emphasized for $CeRu_4Sn_6$. The resulting sphere-like $[Ru_4Sn_6]$ cluster units form a tetragonal body centered packing via common tin atoms. For clarity only one layer is shown. In Ru_2Sn_3 the $RuSn_6$ octahedra are linked by edges and corners while only corner sharing is observed in $Ru_3Sn_{15}O_{14}$. The related stannide $LaRuSn_3$, however, is built up of trigonal prisms which are three-dimensionally connected via all corners.

Ru–Sn distances in this compound range from 251 to 262 pm. Extended Hückel band structure calculations for $Ru_3Sn_{15}O_{14}$ (34) have shown that the Ru–Sn interactions are the strongest in this compound.

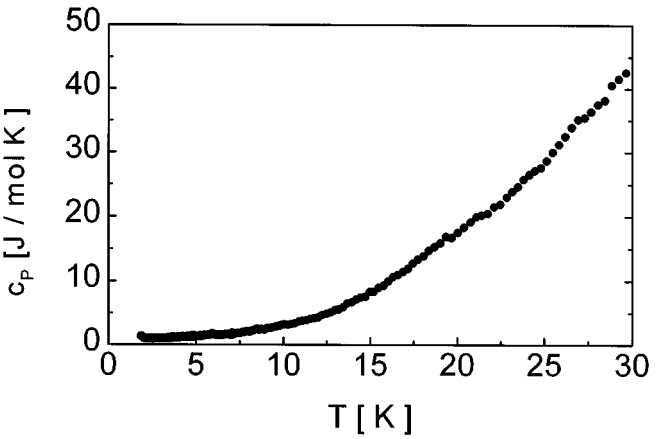

FIG. 4. Temperature dependence of the heat capacity of $CeRu_4Sn_6$.

Condensed $RuSn_6$ units also occur in $LaRuSn_3$ (10); however, in this stannide the tin atoms form a trigonal prismatic arrangement around the ruthenium atoms with Ru–Sn distances of 267.0 pm. These trigonal prisms are connected via common corners with six other prisms forming a three-dimensional $[RuSn_3]^{3-}$ polyanion in which the lanthanum atoms are embedded. A cutout of this polyanion is also shown in Fig. 3.

Physical Properties

Our earlier electrical resistivity measurements (20) show the characteristics of a non-magnetic Kondo lattice. The value of the Curie–Weiss temperature obtained from the plot of the inverse susceptibility *vs* temperature is extremely negative (< -100 K). In the absence of magnetic ordering, the large negative value is significant for the dominance of the Kondo effect. This conclusion suggests that $CeRu_4Sn_6$

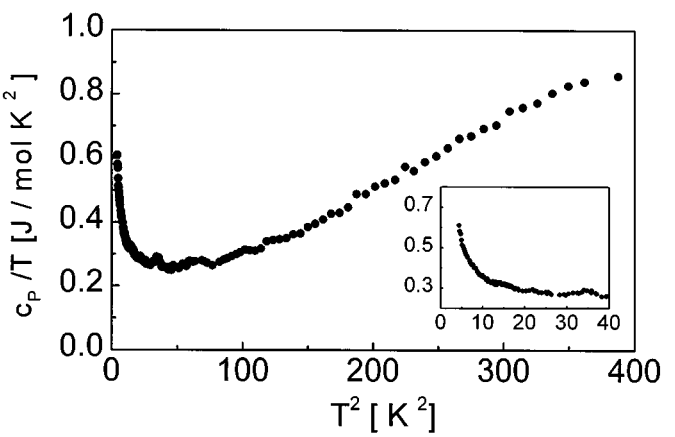

FIG. 5. Plot of C/T vs T^2 for $CeRu_4Sn_6$ with the low-temperature data shown in the inset.

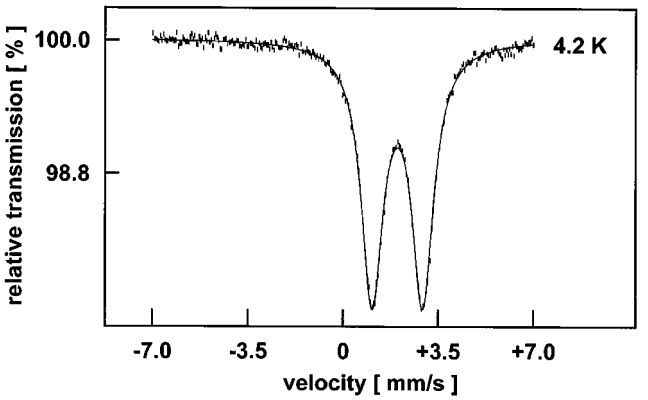

FIG. 6. Experimental and simulated ^{119}Sn Mössbauer spectrum of $CeRu_4Sn_6$ at 4.2 K relative to $CaSnO_3$.

might be a heavy-fermion compound. In order to prove this idea in more detail, heat capacity measurements were performed. No lambda type anomaly characteristic for magnetic ordering was observed in the temperature range from 2 to 30 K (Fig. 4). The plot of C/T vs T^2 shown in Fig. 5 is almost linear in the interval 10–20 K and the linear coefficient (γ) for the heat capacity amounts to about 40 mJ/mol K^2. At 2 K, the C/T vs T curve reaches its maximum of about 600 mJ/mol K^2 after flattening around 275 mJ/mol K^2 in the temperature range 4–10 K. Such large C/T values are frequently observed for heavy-fermion systems (35, 36).

The ^{119}Sn Mössbauer spectra recorded at 4.2 and 78 K are essentially identical. The 4.2 K data are presented in Fig. 6. Although the structure contains two crystallographically different tin sites with a site occupancy ratio of 2:1 (Fig. 2), we observe only a single Mössbauer signal at an isomer shift $\delta = 2.00(8)$ mm/s for $CeRu_4Sn_6$ at 4.2 K. This signal is subjected to a significant quadrupole splitting of $\Delta Eq = 1.98(2)$ mm/s with a slightly elevated line width of $\Gamma = 0.96(2)$ mm/s. Since both peaks of the present spectrum have the same intensity, the signals of the two chemically similar tin sites must be superimposed, leading to the enlarged line width. The large quadrupole splitting reflects the low site symmetry of the two tin positions (Fig. 2). In related stannides with higher site symmetry for the tin atoms, the quadropule splitting is less pronounced (37, 38).

ACKNOWLEDGMENTS

We are indebted to Professors Hellmut Eckert and Wolfgang Jeitschko for their interest and support of this work. We thank Dipl.-Ing. Ute Rodewald for the data collection and Klaus Wagner for the EDX investigations. This work was financially supported by the Deutsche Forschungsgemeinschaft and the Fonds der Chemischen Industrie.

REFERENCES

1. O. Schwomma, H. Nowotny, and A. Wittmann, *Monatsh. Chem.* **95,** 1538 (1964).
2. C. P. Susz, Thesis No. 1758, Université de Genève, Switzerland, 1976.
3. L. Perring, P. Feschotte, and J. C. Gachon, *Thermochim. Acta.* [submitted].
4. L. Perring, P. Feschotte, F. Bussy, and J. C. Gachon, *J. Alloys Compd.* **245,** 157 (1996).
5. O. Nial, *Svensky Kem. Tidskr.* **59,** 172 (1947).
6. D. J. Poutcharovsky, K. Yvon, and E. Parthé, *J. Less-Common Met.* **4,** 139 (1975).
7. T. Söhnel, W. Reichelt, U. Kreyßig, G. Behr, "8. Vortragstagung, Fachgruppe Festkörperchemie der GDCh, PII 47, 20.-22. 03. 1996, Darmstadt, Germany".
8. O. Schwomma, H. Nowotny, and A. Wittmann, *Monatsh. Chem.* **94,** 681 (1963).
9. V. Sechovsky, L. Havela, L. Neuzil, A. V. Andreev, G. Hilscher, and C. Schmitzer, *J. Less-Common Met.* **121,** 169 (1986).
10. B. Eisenmann and H. Schäfer, *J. Less-Common Met.* **123,** 89 (1986).
11. T. Fukuhara, I. Sakamot, and H. Sato, *J. Phys. Condensed Matter* **3,** 8917 (1991).
12. J. L. Hodeau, J. Chenavas, M. Marezio, and J. P. Remeika, *Solid State Commun.* **36,** 839 (1980).
13. G. P. Espinosa, *Mater. Res. Bull.* **15,** 791 (1980).
14. A. S. Cooper, *Mater. Res. Bull.* **15,** 799 (1980).
15. G. P. Espinosa, A. S. Cooper, H. Barz, and J. P. Remeika, *Mater. Res. Bull.* **15,** 1635 (1980).
16. G. P. Espinosa, A. S. Cooper, and H. Barz, *Mater. Res. Bull.* **17,** 963 (1982).
17. D. M. Vandenberg, *Mater. Res. Bull.* **15,** 835 (1980).
18. S. Miraglia, J. L. Hodeau, F. de Bergevin, and M. Marezio, *Acta Crystallogr. B* **43,** 76 (1987).
19. G. Venturini, B. Chafik El Idrissi, J. F. Marêché, and B. Malaman, *Mater. Res. Bull.* **25,** 1541 (1990).
20. I. Das and E. V. Sampathkumaran, *Phys. Rev. B* **46,** 4250 (1992).
21. K. Yvon, W. Jeitschko, and E. Parthé, *J. Appl. Crystallogr.* **10,** 73 (1977).
22. G. M. Sheldrick, "SHELX-86, Program for the Solution of Crystal Structures," University of Göttingen, Germany, 1986.
23. G. M. Sheldrick, "SHELXL-93, Program for Crystal Structure Refinement," University of Göttingen, Germany, 1993.
24. H. D. Flack, *Acta Crystallogr. A* **39,** 876 (1983).
25. G. Bernadinelli and H. D. Flack, *Acta Crystallogr. A* **41,** 500 (1985).
26. I. R. Harris and G. V. Raynor, *J. Less-Common Met.* **9,** 7 (1965).
27. E. Teatum, K. Gschneidner, Jr., and J. Waber, Rep. LA-2345, U.S. Department of Commerce, Washington, DC, 1960.
28. J. X. Boucherle, F. Givord, P. Lejay, J. Schweizer, and A. Stunault, *Acta Crystallogr. B* **44,** 377 (1988).
29. M. Bonnet, J. X. Boucherle, F. Givord, F. Lapierre, P. Lejay, J. Odin, A. P. Murani, J. Schweizer, and A. Stunault, *J. Magn. Magn. Mater.* **132,** 289 (1994).
30. L. Pauling, "The Nature of the Chemical Bond and The Structures of Molecules and Crystals". Cornell Univ. Press, Ithaca, NY, 1960.
31. J. Donohue, "The Structures of the Elements", Wiley, New York, 1974.
32. T. Wölpl and W. Jeitschko, *J. Alloys Compd.* **210,** 185 (1994).
33. A. Lang and W. Jeitschko, *J. Mater. Chem.* **6,** 1897 (1996).
34. W. Reichelt, T. Söhnel, O. Rademacher, H. Oppermann, A. Simon, J. Köhler, and Hj. Mattausch, *Angew. Chem.* **107,** 2307 (1995).
35. F. Steglich, *J. Phys. Chem. Solids* **50,** 225 (1989).
36. H. R. Ott, *Progr. Low Temp. Phys.* **11,** 215 (1987).
37. F. Mirambet, B. Chevalier, L. Fournès, P. Gravereau, and J. Etourneau, *J. Alloys Compd.* **203,** 29 (1994).
38. P. Gravereau, F. Mirambet, B. Chevalier, F. Weill, L. Fournès, D. Laffargue, F. Bourée, and J. Etourneau, *J. Mater. Chem.* **4,** 1893 (1994).